



Carbonatite ring-complexes explained by caldera-style volcanism

SUBJECT AREAS:

SEISMOLOGY

VOLCANOLOGY

PETROLOGY

STRUCTURAL GEOLOGY

Magnus Andersson¹, Alireza Malehmir¹, Valentin R. Troll¹, Mahdieh Dehghannejad¹, Christopher Juhlin¹ & Maria Ask²

¹Department of Earth Sciences, Uppsala University, Uppsala, Sweden, ²Department of Civil, Environmental and Natural Resources Engineering, Luleå University of Technology, Luleå, Sweden.

Received
8 January 2013

Accepted
3 April 2013

Published
17 April 2013

Correspondence and requests for materials should be addressed to A.M. (alireza.malehmir@geo.uu.se)

Carbonatites are rare, carbonate-rich magmatic rocks that make up a minute portion of the crust only, yet they are of great relevance for our understanding of crustal and mantle processes. Although they occur in all continents and from Archaean to present, the deeper plumbing system of carbonatite ring-complexes is usually poorly constrained. Here, we show that carbonatite ring-complexes can be explained by caldera-style volcanism. Our geophysical investigation of the Alnö carbonatite ring-complex in central Sweden identifies a solidified saucer-shaped magma chamber at ~3 km depth that links to surface exposures through a ring fault system. Caldera subsidence during final stages of activity caused carbonatite eruptions north of the main complex, providing the crucial element to connect plutonic and eruptive features of carbonatite magmatism. The way carbonatite magmas are stored, transported and erupt at the surface is thus comparable to known emplacement styles from silicic calderas.

Carbonatites are rare carbonate-rich magmatic rocks that are usually associated with alkaline silica-undersaturated intrusions. Although they make up a very small portion of the crust's volume, they occur in all continents from Archaean to the present and are of great relevance for our understanding of crustal and mantle processes. The Alnö complex is one of only several tens of known alkaline and carbonatite ring-intrusions in the world (see Supplementary Table S1) and is the type-locality for the rock type *alnöite*^{1–3}. The intrusion was emplaced at 584 ± 7 Ma⁴ into Palaeoproterozoic country-rock and comprises melilite-bearing mafic and alkaline dyke rocks (nephelinites, ijolites, pyroxenites and carbonatites). In addition, carbonate-cemented vent-breccias with accretionary lapilli provide evidence for associated volcanic activity⁵. Alnö's deeper plumbing system, and that of most other carbonatite ring-complexes, remains poorly constrained, however, leaving us with considerable uncertainties as to how the plutonic and the volcanic environments in carbonatite centres connect. Here, we present three high-resolution reflection seismic, gravity, and ground magnetic profiles across the Alnö igneous complex to better understand the internal structure of the intrusion at depth. Our findings identify a saucer-shaped magma chamber at ~3 km depth below the present day land surface, from the shoulders of which the majority of carbonatite dykes were injected into the overlying alkaline silicate rocks as moderately- to steeply-dipping sheets. Caldera subsidence during the final stage of activity caused carbonatites to erupt north of the main complex, providing the crucial elements to link plutonic and eruptive aspects of carbonatite magmatism at Alnö. This helps us to better understand the way carbonatite magmas are stored, transported and how they erupt at the surface.

Carbonatites frequently occur in ring-complexes, cf. Supplementary Table S1, and have been related to e.g., stable cratonic regions, orogenies, rifting and extension within continental margins, and to mantle plumes^{3,6–10}. They have been found in all continents with the Kaiserstuhl volcanic complex in the Rhine graben⁷ and the Oldoinyo Lengai volcano in the East African Rift Valley⁸ being the youngest examples. The latter is the only known active carbonatite volcano, albeit of unique composition⁶. As most carbonatites are known from plutonic complexes and only a few volcanic examples are available, there is a significant gap in our understanding of the plutonic-eruptive association for this unusual group of rocks as plutonic and eruptive episodes are rarely preserved side by side¹¹. The aim of this study is to link the plutonic and volcanic occurrence of carbonatites at Alnö (Fig. 1) to provide a better understanding of storage and transport of carbonatite magmas by constraining the magmatic plumbing system at depth.

The Alnö complex is coeval with the Fen carbonatite complex in southern Norway (583 ± 15 Ma via ⁴⁰Ar/³⁹Ar dating)¹², although they are some 600 km apart. It has been suggested that they are genetically linked⁴ and a palaeo-rift could also link carbonatites in the Kola Peninsula to Alnö and Fen (Fig. 1)^{4,13,14}. However, most intrusions in Kola are either younger (~380–360 Ma) or older (Palaeoproterozoic)^{6,15}, making it likely that Alnö and Fen belong to a separate event.

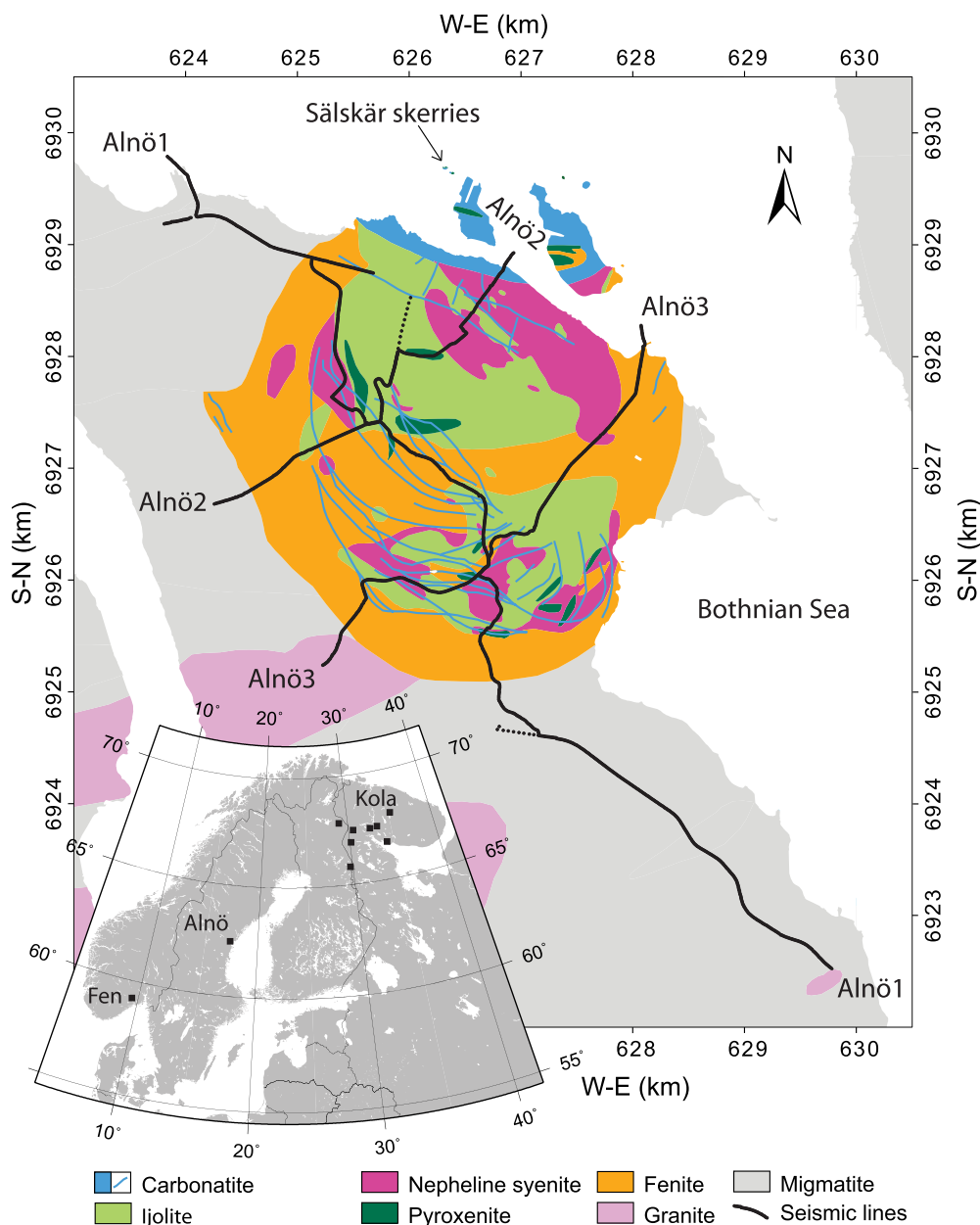


Figure 1 | Geological map of the Alnö alkaline and carbonatite ring complex¹⁶. Inset map shows locations of the Alnö complex in central Sweden, the coeval Fen complex in Norway and the alkaline and carbonatite intrusions of the Kola Peninsula. Locations of the reflection seismic profiles (Alnö1, 2 and 3) are shown. Additional source points were activated off the seismic profiles to increase seismic resolution at locations where there were access limitations and restrictions. Extrusive activity is preserved in the Sälskär skerries. Geological map is kindly provided by the Geological Survey of Sweden.

The island of Alnö hosts the 584 ± 7 Ma⁴ semi-circular Alnö intrusive complex that shows a radius of ~ 2.5 km in the northernmost part of the island. It is one of the less than 500 documented alkaline-carbonatite and carbonatite intrusions and it is one of the largest carbonatite ring-complexes; of the latter only several tens are known (Supplementary Table S1). In addition, Alnö makes a rare case due to its intrusive-extrusive carbonatite association^{5,16}. The main portion of the Alnö igneous complex contains a suite of alkaline silicate rocks (ijolite, nepheline-syenite, and pyroxenite) and various carbonatite and silicate-carbonatite dykes (sövites and silico-sövites respectively) that crop out in a semi-circular pattern (Fig. 1)^{17–19}. Alnöite, a mafic alkaline silicate rock that belongs to the kimberlite family and is melilite-rich, has been named after the island^{16,17}. In the 1980s, the diamond potential at Alnö was investigated but without significant results²⁰. The carbonatites at Alnö also occur dominantly

as dykes and have been divided into two groups with respect to their size and dip direction¹⁶. The longer and thicker dykes are restricted to the southern part of the intrusion and generally dip outward from the centre, whereas shorter and thinner dykes dip dominantly inward towards the centre of the complex. A suite of radial dykes is present as well, which from field mapping is thought to be the oldest group of dykes^{17,18}. The term ‘dyke’ is used here in a general sense, not necessarily indicating that the dip is vertical, but rather that it is of an orientation steeper than 45° . Migmatites and gneisses, the country-rocks to the complex, have been metasomatised to fenites through fluid-rock interaction in a 500–600 m wide zone²¹. Finitization added Na_2O , K_2O , CaO , MgO and FeO and reduced SiO_2 in the migmatite country rocks, while SiO_2 was added to the carbonatites to make silico-sövites^{21–23}. An approximate overburden of 0.5–1 km is estimated to have been eroded from the complex since the time of



its emplacement¹⁸, but breccias with carbonatite and kimberlite clasts and accretionary lapilli contained in a matrix of flow-banded carbonatite occur in the Sälskär skerries 700 m north of Alnö Island (Fig. 1), recording an explosive volcanic vent in this region^{5,16,24}.

On the basis of available radiometric ages, intrusive emplacement at Alnö likely took several million years³, and two scenarios for the emplacement of the intrusion and its associated carbonatite dykes are currently available^{17,18}. So far, neither depth constraints nor geophysical data have been available to validate either of the rival views. Although the complex is relatively poorly exposed, the combination of earlier work and the presented geophysical data make Alnö likely the structurally best-characterized carbonatite complex in the world at present.

The first and older of the existing emplacement models suggest an intrusion centre about 1 km north of Alnö Island that created four sets of inward dipping cone sheet swarms, with focal points at different depths below the current erosion surface (1, 2, 3.5, and 7–8 km respectively)^{17,25}. Two sets of radial dykes were reported to relate to focal depths of 2 km and 7–8 km below the surface, respectively, and a main magma feeding reservoir at 9–10 km depth was proposed^{17,25}. Later, detailed geological mapping was employed to reduce the depth extent of the intrusion from ~10 km to 2–3 km resulting in an altogether different emplacement model¹⁸. Carbonatite dykes dipping outward from the centre of the intrusion were found to be almost as common as inward dipping ones and a shallow dome-shaped magma chamber, with a roof about 2 km below the palaeo-surface was inferred to have supplied the steeply dipping radial dykes and the shallowly dipping cone sheets¹⁸. Concentric outward-dipping carbonatite dykes (ring-dykes) formed along post-doming subsidence-related fault structures¹⁸. This emplacement model hence postulates initial up-doming followed by caldera subsidence caused by a single magma chamber that underlies Alnö at shallow depth, and which was the main source of the Alnö ring-complex. We will refer to these two models according to the proponents that put them forward,

the older as the “von Eckermann-model” and the younger as the “Kresten-model”.

Results

To investigate the deep structure at Alnö, we acquired high-resolution reflection seismic, gravity and magnetic data along three profiles, totalling about 17 km in length (Fig. 1); Alnö1 about 9 km long (NW-SE direction), Alnö2 and Alnö3, each about 4 km long (SW-NE direction). The latter two profiles (Alnö2 and Alnö3) are semi-parallel to each other and cross Alnö1. Alnö1 starts on the country rocks south of the main intrusion, crosses the main intrusion and ends on the country rocks again in the north. Alnö2 and Alnö3 start on the country rocks in the southwest and end about 250 m out on the sea ice (at the time of the survey). Seismic data quality in all three profiles is generally good with clear reflections already observed in some raw shot gathers (see Supplementary Fig. S1). Gravity and ground magnetic data were measured along the seismic profiles prior to the seismic data acquisition. Gravity data were collected at 100 m intervals while magnetic data were collected every 1–2 m. In addition, petrophysical measurements were performed on samples of various rock types from the area (Fig. 2). These measurements suggest that the majority of carbonatites have low velocity and density in comparison with the alkaline rocks.

Gravity and magnetic fields both increase over the intrusion and gravity data show a rapid climb of about 20 mGal over the intrusion (Figs. 3 and 4). For the magnetic data, a positive anomaly of 4000 nT is observed and the gravity field anomaly is flat and constant over the centre of the intrusion (see Fig. 3 and Supplementary Fig. S2). The magnetic data, in turn, show pronounced jumps at locations where carbonatite and associated alkali-silicate dykes are known from geological records. The carbonatite dykes are usually rich in magnetic minerals such as pyrochlore, therefore, they show high magnetic susceptibility which is probably causing the short wavelength magnetic anomalies observed in Figs. 3 and 4. The long magnetic

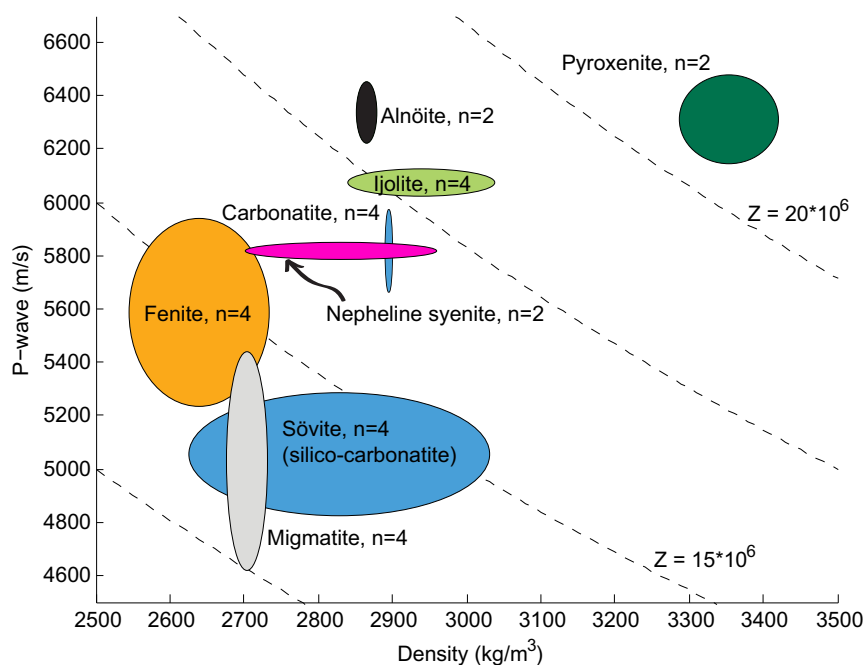


Figure 2 | Velocity-density graph for samples collected from Alnö Island. Most velocities were measured while samples were pressurized at 65 MPa. The acoustic impedance contrast between alkaline rocks, country rock migmatite and carbonatite is high, suggesting that reflections are generated if these rock types are juxtaposed. For example, jumps in the magnetic data correlate with the reflections observed on the seismic images (see Fig. 3 and Supplementary Fig. S2) and, at many locations, these magnetic highs are associated with carbonatite dykes mapped at the surface. This is consistent with our interpretation of the petrophysical measurements that carbonatites have a significant acoustic impedance contrast against most other lithologies in the study area. Number of samples used in the measurements is shown by “n” in the plot.

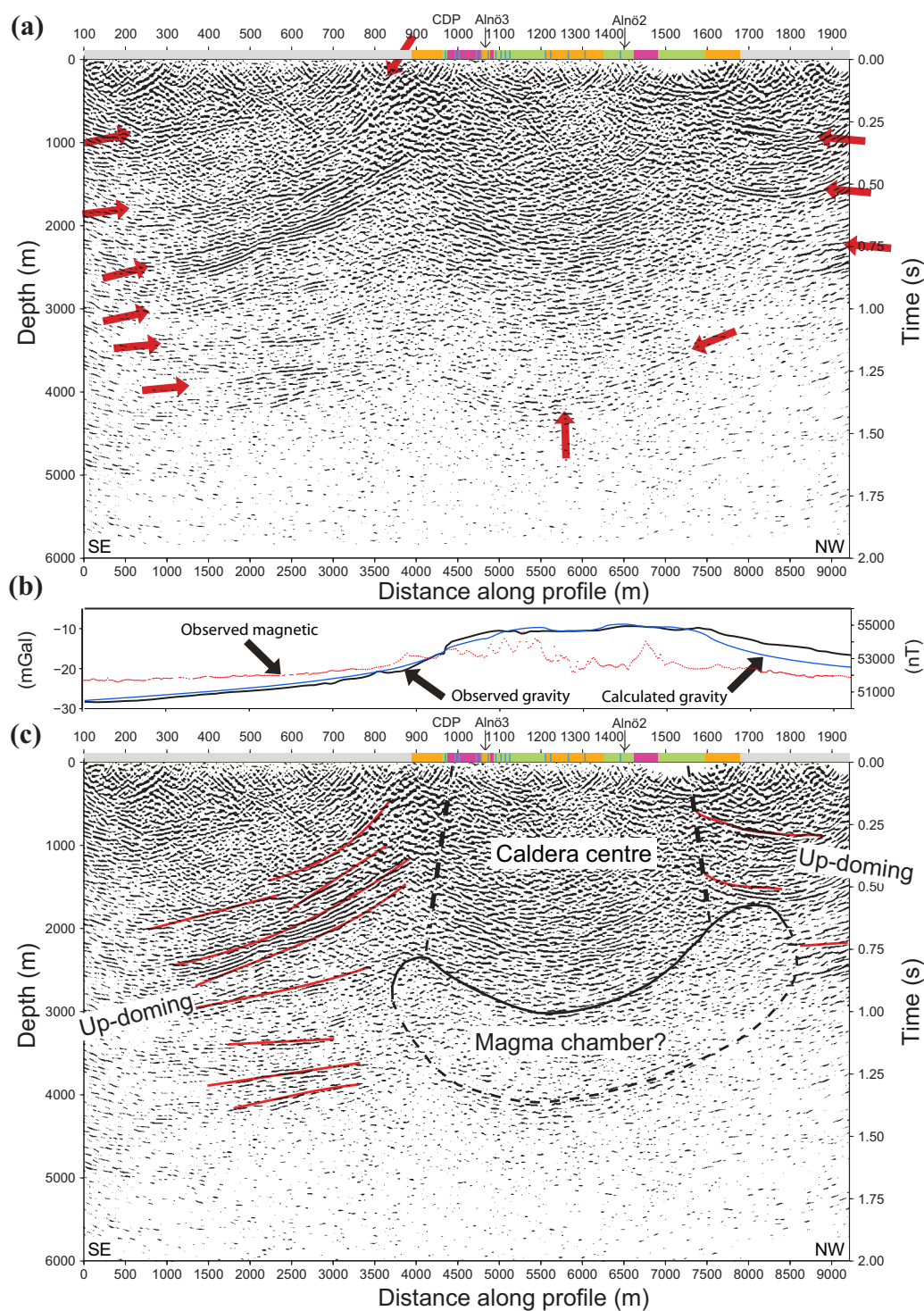


Figure 3 | Post-stack depth migrated seismic section, measured, and forward calculated (see Supplementary Fig. S3), gravity and magnetic data along Alnö1 ((a) uninterpreted; (b) gravity and magnetic data; (c) interpreted). Surface geology (as in Fig. 1) is shown along the top of the seismic profile. A complex reflectivity pattern extends down to a depth of about 3 km between Common Depth Points (CDPs) 900–1500. The transparent zone below this depth represents the location of the magma chamber from which carbonatite dykes were fed. Gently to steeply dipping reflections observed in the southern and northern parts of Alnö1 represent up- doming structures (solid red lines) associated with a saucer-shaped like magma chamber. The boundary between the dipping reflectors outside the igneous complex and the chaotic interior is marking the position of the main ring-fault system (steep dashed black lines). A good correspondence between deeper reflective zones is also observed in Alnö2 and Alnö3 (see solid black lines in Figs. 4c and 4f). Note that carbonatite dykes correlate with the measured magnetic jumps, for example between CDPs 1000 and 1200. The 2.5D forward gravity modelling along the seismic profiles supports the seismic interpretation that the main intrusion (former magma chamber) has a maximum vertical extent of ~1 km and resides at depth of about 3 to 4 km (see also Supplementary Figs. S3 and S4).

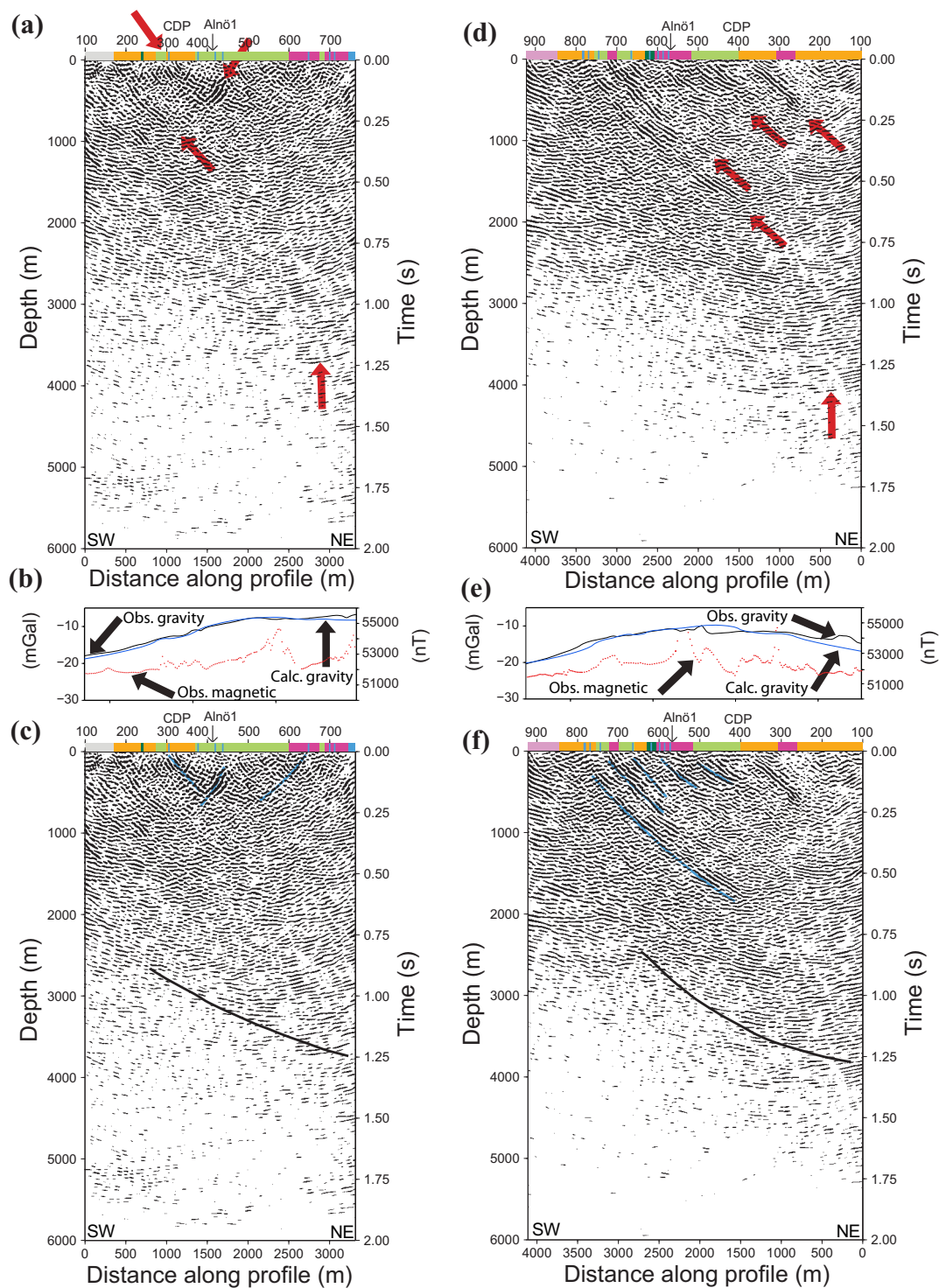


Figure 4 | Post-stack depth migrated seismic section, measured, and forward calculated, gravity and magnetic data along Alnö2 and 3 ((a) and (d) uninterpreted; (b) and (e) gravity and magnetic data; (c) and (f) interpreted). Surface geology (as in Fig. 1) is shown along the top of the seismic profile. Note that carbonatite dykes are well picked out by the seismic data (solid blue lines) and correlate with the measured magnetic jumps, for example at the northeasternmost part of the Alnö2 or at about CDP 400 and CDPs 750 to 800 in Alnö3. The 2.5D forward gravity modelling along the seismic profiles supports the seismic interpretation that the intrusion extends down to about 3 to 4 km depth (see Supplementary Fig. S4b and S4d).

wavelength anomaly observed over the main intrusion represents the bulk effect of the entire intrusion.

A good correlation between the magnetic peaks and seismic reflections is evident at points where steeply dipping reflectors project to the surface, for example CDPs 1000–1100 in Fig. 3c, CDP 300 in Fig. 4c, and CDPs 500–800 in Fig. 4f. This correlation demonstrates that most of the strong reflectors originate from carbonatite dykes.

Tables 1 and 2 summarize the main seismic data acquisition and processing parameters. Processing results show numerous reflections with various dips that range from flat lying to steeply dipping. In several locations these reflections project to the surface and allow correlation with surface geology. Alnö1 shows a strongly reflective zone down to about 2.5 km depth at the centre of the intrusion, below which the reflectivity becomes weak with signs of flat to gently



dipping reflections only (Fig. 3a). A general pattern of flat lying reflections from 4.5 km depth to steeply dipping reflections closer to the surface is characteristic of the data along this line. The reflectivity is rather chaotic in the central part of the main intrusion and contains short segments of reflections that have opposite dips. In the northern parts of the profile, reflections mainly dip northwest and appear to be dipping moderately. Below 2.5 km depth, structures are mainly transparent except in the southeastern parts of the main intrusion where some 3–4 km long reflections are observed. Although discontinuous, these reflections have a gentle topography (see also Supplementary Fig. S2a), potentially representing an up-doming structure or the top of the magma chamber. At about CDP 900–1000, a narrow transparent zone is observed at which two oppositely dipping reflectivity patterns are observed at about 1.5 km depth. Due to the complexity of the geology (Fig. 1), most reflections, except the steeply dipping ones, likely show apparent dips and their true dips are much larger than seen in the seismic images.

Alnö2 in comparison with the other two lines shows the least number of reflections. However, at least two sets of steeply dipping reflections extend to the near surface (Fig. 4a and Supplementary Fig. S2b). The strongest reflections dip towards the northeast and, in parts, migrate out of the seismic section. Again, the reflectivity continues down to a depth of about 2.5–3.0 km at which the steeply reflectivity becomes flat lying to gently dipping (Fig. 4c; see the stacked section as well; Supplementary Fig. S2b). With a few exceptions, reflections dip mainly outwards inside the main intrusion. These reflections in the southwestern part of the profile are associated with a few carbonatite dykes and contacts between fenite and the pyroxenite (Fig. 1), but in the northeastern part of the profile they occur at the contact between the nepheline syenite and ijolite rocks where very few thin carbonatite dykes are mapped on the surface geology. Again, most of the reflections correlate well with the magnetic highs that sometimes represent a carbonatite dyke and sometimes contacts between ultramafic rocks and less mafic rocks. A magnetic high observed at the northeastern margin of the line (Fig. 4b) is a clear response from a thick (c. 50 m) carbonatite dyke. As also evident from the surface geology, the gravity data indicate the intrusion extends further towards northeast (Fig. 4b).

Table 1 | Main acquisition parameters for the reflection seismic survey, March 2011

Parameter	Unit
<i>Survey parameters</i>	
Type of survey	Two-dimensional crooked line
Recording system	SERCEL 408 XL
Spread geometry	Split-spread geometry (60 stations tailing)
No. of active channels	360
Maximum offset	Alnö1: 2.8 km, Alnö2: 2.1 km, Alnö3: 2.5 km
Profile length	Alnö1: 9 km, Alnö2: 3.5 km, Alnö3: 4 km
Source type	VIBSIST-3000
Nominal CDP fold	Alnö1: 180, Alnö2: 180, Alnö3: 180
<i>Spread parameters</i>	
Receiver spacing	10 m
Source interval	10 m
Recording length	30 s (3 s after decoding)
Sampling rate	1 ms
<i>Receiver and source parameters</i>	
Geophone frequency	28 Hz
Geophone per set	Single
No. of sweeps	3–5
No. of shots	Alnö1: 783, Alnö2: 306, Alnö3: 388

Table 2 | Principal processing steps used to process the seismic data

Step	Parameters
1	Read 30 s uncorrelated seismic data
2	Data decoding and reduction to 3 s
3	Build geometry data
4	Trace editing
5	Pick first breaks: full offset range, both manual picking and automatic neural network algorithm with manually inspection and correction
6	Refraction static and elevation static corrections: datum 100 m, replacement velocity 5500 m/s, v_0 1000 m/s
7	Geometric-spreading compensation: v^2t
8	Band-pass filtering: 20-30-160-180 Hz
9	Surface-consistent deconvolution: filter 150 ms, gap 14 ms, white noise 0.1%
10	Band-pass filtering: 20-30-160-180 Hz
11	Top mute: 30 ms after first breaks
12	Direct shear wave attenuation (near-offset)
13	Air blast attenuation
14	Trace balance using data window
15	Velocity analysis (iterative)
16	Residual static corrections (iterative)
17	Normal moveout corrections (NMO): 30% stretch mute
18	Stack
19	f_x -deconvolution (poststack coherency filter)
20	Trace balance: 0–3000 ms
21	Finite-difference migration: constant velocity of 6000 m/s
22	Time-to-depth conversion: constant 6000 m/s

Seismic data along Alnö3 (Fig. 4d) show mainly a series of strong parallel steeply northeast dipping reflections that almost all extend to the surface (see also Supplementary Fig. S2c), but also a few weak and deeper southeasterly dipping ones at about 2.5 km depth where again the reflectivity becomes weak flat lying to gently dipping. These reflections are mainly moderately dipping in the central part of the intrusion since the profile is oblique to the structure and, in some cases, parallel to the structure (Fig. 1). Cross-dip analysis²⁶ of the data suggests the presence of southwest dipping reflections at about 2.5 km. Nevertheless, dip directions observed in the profile are different from those observed in Alnö1. This difference can be due to the complex geometry of the carbonatite dykes and the crookedness of the line (Fig. 1). Again, the majority of the steeply dipping reflections extend to the near surface and are associated with the observed magnetic highs, and in one case to a short-wavelength gravity jump (Fig. 4e and 4f). These reflections correlate well with the locations of carbonatite dykes observed at the surface. Comparison between the reflectivity patterns in Alnö1 and Alnö3 suggests a deeper reflective zone in the eastern part of the intrusion than in its western parts. This is a good indication that these reflections are associated with dense magnetic bodies.

In summary, all three profiles show a strong reflectivity pattern down to about 3 km, deeper in the central part of the complex, where the high reflectivity terminates at a flat lying or transparent zone. Flat lying and deeper reflections down to 4.5 km, although weak, suggest that this termination in the reflectivity is not due to the source penetration and can represent the geology. A high reflectivity zone down to ~3 km depth was identified, which is at its maximum vertical extent beneath the centre of the volcanic complex (Fig. 3a). The shallow part below the centre of the intrusion shows several steeply dipping reflectors, but no clear focal points and/or sheet structures are identified.

Discussion

We interpret the central diffuse reflection pattern to represent a shattered and sunken central caldera block that extends down to a



depth of about 2.5 to 3 km, since no clear and coherent structure with sufficient acoustic contrast is present. The seismically transparent zone below this region (CDPs 800–1700 in Fig. 3c) is attributed to the palaeo-magma reservoir/chamber that is likely the location of a mixed carbonatite-silicate pluton today. The top surface is saucer shape and marks the location from which the carbonatite dykes originate. Although the lower limit is poorly defined, gravity data imply a maximum depth continuation to about 4 km, i.e. a thickness of not more than about 1 km for this body. An initial up-doming pattern is evident from the reflectivity that begins with flat lying reflections at about 4 km depth, grading into steeply dipping reflections closer to the surface (Fig. 3a). The reflectivity pattern shows more reflections in the centre than in the outer part of the complex and the saucer-shaped intrusion shows a somewhat larger lateral extent than the centre's exposure at the surface. In addition, a gravity high in the central part of the intrusion (Fig. 3b) and theoretical studies in magma propagation^{27–32} are consistent with the seismic interpretation. Analogue experiments and field observations have shown that magma will propagate upwards at the edges of sill intrusions once the length to depth ratio of the sill exceeds three³⁰, consistent with our interpretation of a shallow and laterally extensive pluton beneath Alnö.

Although low-viscosity magmas, such as those associated with carbonatite intrusions⁸, likely create saucer-shaped intrusions at shallower depth³⁰, the seismic data image only the subsurface rock geometry at the present day. Thus, it is not clear if the magma chamber formed with a saucer shape during its initial emplacement or if this geometry formed as a result of later large-scale caldera collapse. Irrespective of the initial chamber geometry, our results suggest that a main sill-like magma chamber was situated at about 3.5–4 km depth if an overburden of ~1 km is added. The thickness of this former chamber may also be approximated from the geometry of the up-domed country rocks to the intrusion. Using the country rock reflections observed in the seismic data (Fig. 3c), an estimation of the uplift can be achieved. The inclination of the reflectors projected over the width of the intrusion suggests central uplift of approximately 1 to

1.5 km. While several processes likely influenced this uplift, the 1 to 1.5 km of uplift calculated is broadly consistent with the thickness of the main intrusion derived from the seismic data (Fig. 3c). The up-doming structures observed in the seismic data (Fig. 3c) suggest that the flat to gently dipping reflections are at the contact with the magma chamber at about 3.5 km depth in the southeastern side of Alnö1, but become steeper closer to the surface or at the tip of the intrusion (Fig. 3c). A slightly southeast inclined magma chamber can be envisioned because the gently dipping reflections in the north-western side of Alnö1 appear shallower than the southeastern side.

To test these interpretations and provide constraint on the depth extent of the intrusion, forward modelling of the measured gravity data using the interpretation of the seismic data was carried out. A good fit between the observed and calculated response of the models along all three profiles was achieved (Figs. 3b, 4b and 4e), supporting the interpretation of an intrusion that extends down to 3 to 4 km depth beneath the present-day surface. Our data hence support the “Kresten model”¹⁸, rather than that envisaged by von Eckermann^{17,25}. In fact, no dipping reflections typical of carbonatite dykes are observed in the seismic data below a present day depth of ~3 km (Fig. 3).

Integrating our new results with existing data, emplacement of the Alnö ring-complex began with an alkaline silicate magma rich in dissolved CaCO₃ and associated with CO₂-bearing hydrous fluids²². From Sr-, Pb-, and Nd-isotope data, the mantle source for the Alnö magmas was suggested to have been LREE- and Rb-depleted³³. The magma likely ascended via a weak zone within the migmatite country-rocks, e.g. a fault-zone in an extensional rift setting³⁴, which may have acted as a conduit to allow formation of a sill-like magma chamber at about 3.5–4 km depth below the palaeo-surface. Growth and inflation of this sill-like magma chamber resulted in considerable up-doming at the land surface and initially produced radial tensile and shear fractures around the central intrusion¹⁸ (Fig. 5a). Magma emplacement was associated with intense fenitization of the country rock and rock types such as ijolite, nepheline-syenite, and pyroxenite intruded initially (Fig. 5b). The geometry of the magma chamber at this stage may have been already “lopolithic”, but it is also possible

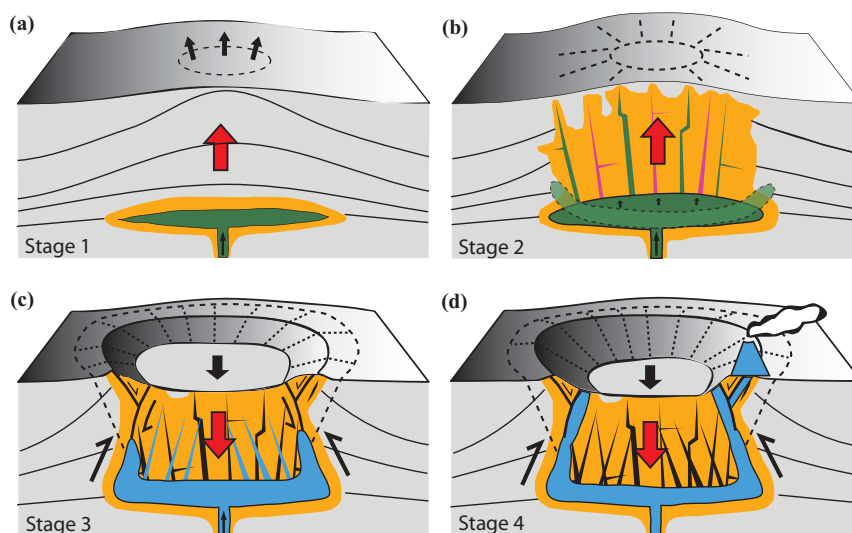


Figure 5 | Schematic model of the emplacement of the Alnö complex. Stage one (a): a low-viscosity silicate magma rich in CaCO₃ ascended and was trapped at about 4–5 km depth. There, it formed a laterally extensive sill-shaped magma chamber. This initiated up-doming and a surface bulge caused early radial dykes to intrude. Stage two (b): growth and inflation of this magma chamber increased tumescence of the overburden. Radial dykes and increasingly inward dipping cone-sheets were intruded into the country-rock above the chamber. Stage three (c): magma, now with a significant carbonatite fraction present, evacuated from the magma chamber via dykes leads to a pressure drop due to material withdrawal causing the central part of the roof to subside. Stage four (d): concentric outward dipping fractures form and are intruded to make ring-dykes during progressive subsidence of the central block/roof during caldera collapse. This likely caused the edges of the main chamber to migrate upwards, at which point further carbonatite dykes were intruded into reverse and normal faults in the caldera periphery, leading to eruption of carbonatite preserved in vent breccias to the north of Alnö Island (indicated to the right in (d)).



that the saucer shape was attained during later collapse. Following the initial emplacement, probably due to magma immiscibility of silicate and carbonatite liquids or fractional crystallization, Alnö produced a volumetrically relevant portion of separate carbonatite magma from the alkaline parent liquids^{8,9,22,35} and a first generation of alnöites and carbonatites intruded the early radial fractures and the cone-sheet fractures during advanced stages of up-doming (cf. Ref. 36). The large concentration of carbonatite dykes in the southern part of the complex (Fig. 1) suggests that the magmatic focus lay beneath this part of the intrusive complex. Progressive dyke intrusions into initially radial and subsequently cone-sheet type fractures led to a pressure drop in the magma reservoir due to chamber evacuation and associated degassing (e.g. Ref. 37). Subsidence along steep to outward dipping faults then set in to form a caldera structure^{18,36,38} (Fig. 5c). A new generation of carbonatite dykes, longer and thicker in nature, then intruded from the margin of the magma chamber into these steep to outward dipping ring-faults to form the ring-type structure of the Alnö complex exposed today cf. Ref. 18 (Fig. 5d). Syn-collapse migration of magma from the main magma reservoir into caldera periphery structures led to satellite intrusions around Alnö Island and triggered the eruption of carbonatite about 700 m north of Alnö Island^{36,39,40} (Fig. 5d). Subsidence of the roof of the magma reservoir thus connects the explosive vents in the northern part of the complex with the shattered central region below Alnö, and with the (saucer-shaped) main magma reservoir at depth, hence linking magma storage, magma transport and eruption at Alnö.

Discussions on the genesis, origin and emplacement of carbonatites have been ongoing for many decades (e.g. Ref. 3,5–10,16–18, 22,35) and documentation of a clear link between plutonic and volcanic environments has mostly proved elusive. Our investigation of the subsurface structure of Alnö helps constrain emplacement scenarios for carbonatite ring-intrusions and dyke swarms and their associated surface volcanism. Alnö is characterized by a ring-type structure associated with a caldera collapse into a shallow, low-viscosity, likely saucer-shaped magma reservoir. Alnö hence evolved through a major caldera cycle, involving up-doming and subsequent subsidence of a shallow crustal magma chamber roof leading to a complex intra-caldera rock association (cf. Ref. 18,36,39). A deep-seated magma chamber some 10 km below the palaeo-land surface as the origin of the carbonatite dykes and volcanism¹⁷ cannot be verified. Alnö is best explained by processes similar to those observed in silicic caldera-type environments where caldera structures are controlled by shallow (<5 km) and frequently sill-like magma chambers^{36,39,40}, but in the Alnö case with an unusual composition. However, the unusual composition seems not to have affected the fundamental volcano-tectonic processes or the broad geometry of traditional caldera volcanism. In addition, the low reflectivity of the interior of the main pluton indicates that there are no significant internal structures within the pluton that can be seismically resolved. Saucer-shaped magma chambers and shallow-level intrusions have recently been found to be widespread, especially when magma intrudes the brittle upper crust (e.g. top 5 km)^{27–32,41}. Our results, therefore, imply that the observed geometry may not be unique to Alnö, but instead may be common to many carbonatite ring-complexes elsewhere (see Supplementary Table S1). On a more local level, a long-lived shallow magma chamber at Alnö would unfavourably have dissolved diamonds as their survival in kimberlite-type magmas is thought to be a function of very rapid ascent¹¹, hence offering an explanation for the unsuccessful diamond exploration. The Alnö carbonatites may, however, be a viable source rock for REEs due to their enriched chemistry⁵, and our data will help to constrain the available REE resources present beneath Alnö Island.

Methods

Petrophysical studies. In order to better understand the seismic response from different rock types, representative samples were collected. While some samples were measured for their P-wave velocity at atmospheric pressure, most samples were

measured at elevated pressures up to 65 MPa. As evidenced from the velocity measurements, fenite and migmatitic rocks show velocities in the range of 5600–5750 m/s (Fig. 2) while ijolite and pyroxenite show much higher velocities. Carbonatite rocks, depending on their exact compositions, show low-to-moderate velocity, although the derived velocities are well within the velocity range (5500–6500 m/s) known from crystalline rocks⁴³. The alkaline igneous rocks show higher seismic velocity (up to about 6400 m/s) compared with the country rocks (about 5100 m/s), see Fig. 2.

The alkaline igneous rocks have densities between 2800 and 3000 kg/m³, in contrast to the country rocks, which show a density more typical of high-silica continental crust (c. 2700 kg/m³). The ring-dyke-forming carbonatites, which sometimes consist of almost pure calcite, have densities similar to that of the country rocks. If carbonatite dykes are rich in magnetic minerals, they show higher density and velocity. The contrast in density and seismic velocity (Fig. 2) generates the reflections from the different rock units. Given the properties established above, we expect particularly strong contrasts between alkaline igneous rocks relative to migmatite country rocks and between carbonatites and alkaline silicate rocks. Carbonatite dykes often contain magnetite, pyrochlore and other opaque phases and, therefore, they frequently show high magnetic susceptibility.

Gravity and magnetic data measurements and modelling. Gravity data were corrected for the equipment drift with a reference station used during the gravity measurements. Locations of the gravity measurements were surveyed using high-precision differential GPS equipment with an accuracy of up to 3 mm on the elevation data. Gravity data were later corrected for topography effects and are presented here as Bouguer gravity anomalies. Magnetic data were corrected for the diurnal effects using a reference station deployed at a relatively calm area and a nearby reference station from the Geological Survey of Sweden. Magnetic data are presented here as total-field magnetic data. An estimation of the thickness of the intrusion can be made with a slab formula assumption²⁶. The main component of the country rock is migmatite (2700 kg/m³) and fenite, which is, metasomatized country rock (2700 kg/m³). In the intrusion area, ijolite (2950 kg/m³) is the dominant silicate igneous rock. Assuming a density contrast of 250 kg/m³ (migmatite vs. ijolite), a depth extent of about 2000 m is required. To complement the seismic data interpretations, 2.5D forward modelling⁴² of the measured gravity data was carried out using a constant density value for each individual body. A good fit between the observed and forward calculated gravity data supports the main intrusion (former magma chamber) to reside between ~3 and 4 km depth. Supplementary Figs. S3b, S4b and S4d show the gravity models used to calculate the responses shown in Figs. 3b, 4b and 4e respectively.

Reflection seismic data acquisition and processing. A nominal receiver and source spacing of 10 m was used for the data acquisition (Table 1). A VIBSIST hammer²⁶ was used to generate seismic signals using 3–5 sweeps at each source location. Additional source points (see Fig. 1) were activated to the side of the seismic profiles to increase seismic fold at locations where there was access limitations and restrictions. Seismic data were acquired during February–March 2011, with about 1–1.5 m snow covering the area. The entire survey lasted about one month, including surveying and staking. Geophones were planted into the frozen ground and this resulted in good geophone coupling and good quality seismic data being acquired. Reflections were immediately visible in some raw shot gathers (Supplementary Fig. S1), which is a characteristic of high quality data in a crystalline environment. Nearly 360 receivers were active during the data acquisition. Alnö1 consisted of 1050 receiver locations and was acquired using an asymmetric split-spread acquisition geometry with about 60 receivers in the tail. Receivers were permanently kept in place during the data acquisition along Alnö2. For Alnö3, 470 receiver locations were used. After 100 shots, receivers were kept permanently in place for the rest of Alnö3. About 25 receivers for each profile were deployed on the sea-ice in order to increase the length of the seismic profiles and potentially extend seismic images past the limits of Alnö Island. No source was activated on sea-ice parts. Analysis of shot gathers recorded close to the sea suggest that the seismic signal is very weak on these receivers, however, weak reflections were observed at these locations after stacking of the data. All source and receiver locations were surveyed using high-precision differential GPS equipment.

Seismic data were processed (Table 2) using conventional pre-stack DMO and post-stack migration algorithms with special focus on the processing steps critical in the crystalline environment such as refraction statics, velocity analysis and source-generated noise attenuation. Cross-dip analysis was also performed to provide information about the potential cross-dip of the reflectors or for improving the seismic images where the seismic lines are crooked. Based on the petrophysical measurements and analysis of first-arrival velocities, a constant velocity of 6000 m/s was used for the time-to-depth conversion. The choice of 6000 m/s could be argued upon, but a slight change of the velocity would have a rather small change on the appearance of the reflections in the profiles. A reflection, which dips 30°, would instead dip 27.9° if 5500 m/s is used, or 32° if 6500 m/s is used. The same reflection would also, if horizontal, be moved 250 meters up and down, respectively, if it was situated at 1 s two-way travel time. Supplementary Fig. S5 shows the effects of different migration velocities on the final appearance of the reflections for the data along Alnö1.

1. Hisinger, W. *Samling till en mineralogisk geografi öfver Sverige* (Nordström, H. A., Stockholm, 1808).



2. Törnebohm, A. E. Mikroskopiska bergartsstudier; XVIII Melilitbasalt från Alnö. *GFF* **76**, 240–251 (1883).
3. Phipps, S. P. Deep rifts as sources for alkaline intraplate magmatism in eastern North America. *Nature* **334**, 27–31 (1988).
4. Meert, J. G., Walderhaug, H. J., Torsvik, T. H. & Hendriks, B. W. H. Age and paleomagnetic signature of the Alno carbonatite complex (NE Sweden): Additional controversy for the Neoproterozoic paleoposition of Baltica. *Precambrian Research* **154**, 159–174 (2007).
5. von Eckermann, H. Boulders of volcanic breccia at the Sälkskär shoals north of Alnö Island. *Arkiv för mineralogi och geologi* **40**, 529–537 (1960).
6. Rukhlov, A. S. & Bell, K. Geochronology of carbonatites from the Canadian and Baltic Shields, and the Canadian Cordillera: clues to mantle evolution. *Miner Petrol* **98**, 11–54 (2010).
7. Le Bas, M. J. *Carbonatite-Nephelinite Volcanism* (Wiley, London, 1977).
8. Fischer, T. P. et al. Upper-mantle volatile chemistry at Oldoinyo Lengai volcano and the origin of carbonatites. *Nature* **459**, 77–80 (2009).
9. Gittins, J. The origin of carbonatites. *Nature* **335**, 295–296 (1988).
10. Wallace, M. E. & Green, H. G. An experimental determination of primary carbonatite magma composition. *Nature* **335**, 343–346 (1988).
11. Gernon, T. M., Brown, R. J., Tait, M. A. & Hincks, T. K. The origin of pelletal lapilli in explosive kimberlite eruptions. *Nature communications* **3** (832), 1–7 (2012).
12. Meert, G. J., Torsvik, T. H., Eide, E. A. & Dahlgren, S. Tectonic Significance of the Fen Province, S. Norway: Constraints from Geochronology and Paleomagnetism. *The Journal of Geology* **106**, 553–564 (1998).
13. van Balen, R. T. & Heeremans, M. Middle Proterozoic–early Palaeozoic evolution of central Baltoscandian intracratonic basins: evidence for asthenospheric diapirs. *Tectonophysics* **300**, 131–142 (1998).
14. Korja, A., Heikkinen, P. & Aaro, S. Crustal structure of the northern Baltic Sea palaeorift. *Tectonophysics* **300**, 131–142 (1998).
15. Downes, H., Balaganskaya, E., Beard, A., Liferovich, R. & Demaiffe, D. Petrogenetic processes in the ultramafic, alkaline and carbonatitic magmatism in the Kola Alkaline Province: A review. *Lithos* **85**, 48–75 (2005).
16. Kresten, P. The Alnö Area (Alnöområdet). In: *Beskrivning till berggrundskartan över Västerbottens län* (Sver. Geol. Und., Uppsala, 1990).
17. von Eckermann, H. *The alkaline district of Alnö island* (Swedish Geol. Surv., Stockholm, 1948).
18. Kresten, P. The Alnö complex; tectonics of dyke emplacement. *Lithos* **13**, 153–158 (1980).
19. Le Maitre, R. W. *Igneous Rocks. A Classification and Glossary of Terms. Recommendations of the International Union of Geological Sciences Subcommission on the Systematics of Igneous Rocks, 2nd ed.* (Cambridge University Press, New York, 2002).
20. Kresten, P. Alnö diamonds. *GFF* **104**, 210 (1982).
21. Morogan, V. & Woolley, A. R. Fenitization at the Alnö carbonatite complex, Sweden; distribution, mineralogy and genesis. *Contrib Mineral Petrol* **100**, 169–182 (1988).
22. Vuorinen, J. H. & Skelton, A. D. L. Origin of silicate minerals in carbonatites from Alnö Island, Sweden: magmatic crystallization or wall rock assimilation? *Terra Nova* **16**, 210–215 (2004).
23. Skelton, A., Hode Vuorinen, J., Arghe, F. & Fallick, A. Fluid-rock interaction at carbonatite-gneiss contact, Alnö, Sweden. *Contrib Mineral Petrol* **154**, 75–90 (2007).
24. Kresten, P. *The Alnö complex: discussion of the main features, bibliography and excursion guide* (Nordic Carbonatite Symposium, Alnö, 1979).
25. von Eckermann, H. Progress of research on the Alnö carbonatite. In: *Carbonatites* (Wiley, New York, 1966).
26. Malehmir, A. et al. Reflection seismic investigations in the Dannemora area, central Sweden: insights into the geometry of poly-phase deformation zones and magnetite-skarn deposits. *Journal of Geophysical Research* **116**, B11307 (2011).
27. Malthe-Sørenssen, A., Planke, S., Svensen, H. & Jamtveit, B. Formation of saucer-shaped sills. *Physical Geology of High-Level Magmatic Systems* **234**, 215–227 (2004).
28. Thomson, K. & Hutton, D. Geometry and growth of sill complexes: insight using 3D seismic from the North Rockall Trough. *Bull Volcanol* **66**, 364–375 (2004).
29. Hansen, D. M. & Cartwright, J. Saucer-shaped sill with lobate morphology revealed by 3D seismic data: implications for resolving a shallow-level sill emplacement mechanism. *Journal of the Geological Society* **163**, 509–523 (2006).
30. Mathieu, L., van Wyk de Vries, B., Holohan, E. P. & Troll, V. R. Dykes, cups, saucers and sills: Analogue experiments on magma intrusion into brittle rocks. *Earth and Planetary Science Letters* **271**, 1–13 (2008).
31. Galland, O., Planke, S., Neuman, E.-R. & Malthe-Sørenssen, A. Experimental modelling of shallow magma emplacement: Application to saucer-shaped intrusions. *Earth and Planetary Science Letters* **277**, 373–383 (2009).
32. Galland, O. Experimental modelling of ground deformation associated with shallow magma intrusions. *Earth and Planetary Science Letters* **317–318**, 145–156 (2012).
33. Andersen, T. Sr, Nd and Pb isotopic data of the Alnö carbonatite complex. Abstract volume. *22nd Nordic Geological Winter Meeting*, 11 (1996).
34. Dahlgren, S. Late Proterozoic and Carboniferous ultramafic magmatism of carbonatitic affinity in southern Norway. *Lithos* **31**, 141–154 (1994).
35. Treiman, A. H. & Essene, E. J. The Oka carbonatite complex, Quebec: geology and evidence for silicate-carbonate liquid immiscibility. *American Mineralogist* **70**, 1101–1113 (1985).
36. Walter, T. R. & Troll, V. R. Formation of caldera periphery faults: an experimental study. *Bull. Volcanol.* **63**, 191–203 (2001).
37. Geshi, N., Shimano, T., Chiba, T. & Nakada, S. Caldera collapse during the 2000 eruption of Miyakejima volcano, Japan. *Bulletin of Volcanology* **64**, 55–68 (2002).
38. Anderson, E. M. Cone-sheets and ring-dykes: The dynamical explanation. *Bulletin of Volcanology* **1**, 135–40 (1937).
39. Troll, V. R., Walter, T. R. & Schmincke, H.-U. Cyclic caldera collapse: Piston or piecemeal subsidence? Field and experimental evidence. *Geology* **30**, 135–138 (2002).
40. Holohan, E. P., Troll, V. R., van Wyk de Vries, B., Walsh, J. J. & Walter, T. R. Unzipping Long Valley: An explanation for vent migration patterns during an elliptical ring fracture eruption. *Geology* **36**, 323–326 (2008).
41. Polteau, S., Mazzini, A., Galland, O., Planke, S. & Malte-Sørenssen, A. Saucer-shaped intrusions: Occurrences, emplacement and implications. *Earth and Planetary Science Letters* **266**, 195–204 (2008).
42. Malehmir, A., Tryggvason, A., Lickorish, H. & Weiheid, P. Regional structural profiles in the western part of the Palaeoproterozoic Skellefte ore district, northern Sweden. *Precambrian Research* **159**, 1–18 (2007).
43. Salisbury, M. H., Harvey, C. W. & Matthews, L. The acoustic properties of ores and host rocks in hardrock terranes. In: *Hardrock Seismic Exploration. Geophysical Development Series No.10* (Society of Exploration Geophysicists, Tulsa, 2003).

Acknowledgments

We acknowledge M. Junge for help with the Supplementary Table S1 and the constructive comments of C. H. Donaldson, C. H. Emeleus, O. Galland, C. Harris, E. P. Holohan, B. Lund, L. Mathieu and B. J. Upton on earlier versions of the manuscript. P. Kresten provided useful information prior to the geophysical data acquisition. Seismic data processing was carried out using Globe Claritas™ and potential field modelling using Model Vision Pro™. The samples were prepared and measured for their density at the Geological Survey of Sweden's laboratory in Uppsala. Seismic velocity measurements were made in the laboratories of Luleå University of Technology and Curtin University. The Swedish Research Council (VR) funded this work.

Author contributions

A.M., M. Ask, V.R.T. and C.J. initiated the project and designed the seismic profiles. A.M. led the fieldwork in Alnö with support by M. Andersson and M.D. M. Andersson, A.M. and M.D. performed the seismic processing and M. Andersson, V.R.T. and A.M. interpreted the results and wrote the manuscript. All authors reviewed the manuscript.

Additional information

Supplementary information accompanies this paper at <http://www.nature.com/scientificreports>

Competing financial interests: The authors declare no competing financial interests.

License: This work is licensed under a Creative Commons Attribution-NonCommercial-NoDerivs 3.0 Unported License. To view a copy of this license, visit <http://creativecommons.org/licenses/by-nc-nd/3.0/>

How to cite this article: Andersson, M. et al. Carbonatite ring-complexes explained by caldera-style volcanism. *Sci. Rep.* **3**, 1677; DOI:10.1038/srep01677 (2013).